

This document is downloaded from DR-NTU, Nanyang Technological University Library, Singapore.

Title	Effect of plating parameters on the intrinsic stress in electroless nickel plating
Author(s)	Chen, Zhong; Xu, Xiaoda; Wong, Chee C.; Mhaisalkar, Subodh Gautam
Citation	Chen, Z., Xu, X., Wong, C. C., & Mhaisalkar, S. G. (2003). Effect of plating parameters on the intrinsic stress in electroless nickel plating. <i>Surface and coatings technology</i> , 167(2-3), 170-176.
Date	2003
URL	http://hdl.handle.net/10220/8175
Rights	© 2003 Elsevier. This is the author created version of a work that has been peer reviewed and accepted for publication by <i>Surface and Coatings Technology</i> , Elsevier. It incorporates referee's comments but changes resulting from the publishing process, such as copyediting, structural formatting, may not be reflected in this document. The published version is available at: [http://dx.doi.org/10.1016/S0257-8972(02)00911-8].

Effect of plating parameters on the intrinsic stress in electroless nickel plating

Zhong Chen¹, Xiaoda Xu, Chee C. Wong, Subodh Mhaisalkar

School of Materials Engineering, Nanyang Technological University, Singapore 639798

Abstract:

With the increasing application of electroless nickel (EN) as a bumping or under-bumping metalization material, the microelectronic packaging engineers are required to have a deeper understanding and control of intrinsic stress in electroless nickel (EN) plating. The purpose of this work is to investigate the effect of some most important operating parameters on the formation of intrinsic stress during plating. The analysis of variances (ANOVA) method was applied to obtain both single effect and compound effect of selected factors. Results indicate that high pH value and aged solution affect the intrinsic stress significantly, while surface roughness does not have much influence on the intrinsic stress for the range investigated. Aging at 190°C for 170 hours changes neither the Ni-P structure nor the intrinsic stress to a significant degree. Further investigation indicated that the intrinsic stress was probably related to the Ni-P microstructure as a result of the deposition rate. It was found that the higher the deposition rate, the higher the intrinsic stress.

¹Corresponding author: Tel: +65-67904256; Fax: +65-67909081

E-mail address: aszchen@ntu.edu.sg (Z. Chen)

Key words:

Electroless nickel plating; Intrinsic stress; Metal turnover (MTO)

1. Introduction

Electroless nickel (EN) plating had shown good potential as a low-cost bumping material for flip chip application. It provides a selective metal deposition directly on the conductor metals such as Al and Cu, therefore lithography and etching processes are saved. EN bumping process has been proven to be acceptable in anisotropic conductive adhesive (ACA) and Non-conductive adhesive (NCA), as well as under bump metallization (UBM). Recently, the microelectronics packaging industry has required that the end users have to understand, and to be able to control its intrinsic stress [1], which is one of most important concerns for bumping reliability.

The internal stress of a deposit usually consists of two parts: extrinsic and intrinsic. Extrinsic stress, or thermal stress, primarily results from the mismatch of coefficient of thermal expansion (CTE) between the deposit and the substrate. Intrinsic stress is formed during the deposition process and is mainly controlled by the composition of the deposition solution and the operation conditions [2].

Researchers have found that the intrinsic stress can be influenced by certain processing parameters; for example, aged solution could severely affect the EN intrinsic stress [3]. However, systematic work is still lacking on the effect of all the key process specifications on the intrinsic stress, even less work has been done on the compound effect of these factors. Most of the investigations focused on the relationship between process parameters and intrinsic stress only. The plated Ni-P microstructures have not been closely observed, which might be able to reveal the connection between properties of plated Ni-P film and its process parameters.

In this work, the analysis of variance (ANOVA) method [4] was applied to investigate the influences of three levels combinations of three selected factors on the formation of EN intrinsic stress. During the investigation, not only single effect, but also interaction effects of selected factors were investigated. Low temperature annealing was carried out to investigate the possible change in the stress due to long time service of the component.

2. Experimental

The electroless Ni-P alloy was deposited on one side of copper foils, 50mm×5mm×0.1mm, for intrinsic stress measurement. A thin layer of lacquer was coated on the opposite side before plating. The copper foils were cleaned in boiled acetone, isopropyl alcohol (IPA), and deionized water (DI) in sequence. Then they were electropolished, or chemically etched. This was to create different surface roughness for the variation of the substrate condition. The surface roughness of the samples was measured by Alpha-Step[®] 500 surface profiler. The electropolished, as-received, and chemically etched copper foils were prepared for the electroless nickel plating as three levels of surface roughness conditions. Before plating, the copper foils were dipped into diluted HCl solution (1:1 in volume ratio with water) for surface activation, followed by DI water cleaning. A pretreated copper strip was then immersed in the electroless nickel (EN) solution at 90°C with stirring. The EN solution used in this study is composed of NiSO₄·7H₂O (0.1M), NaH₂PO₂·H₂O (0.28M), lactic acid (40 ml/L), propionic acid (5 ml/L), NaOH (0.45M), NaAc (0.15M), and a small quantity of additives. Typical weight percentage of phosphorus content in the deposit is around 7% by this recipe.

The developmental intrinsic stress within the Ni-P deposit bends the specimen. Tensile stress in the deposit will bend the specimen to form a concave bow while compressive stress produces a convex bow. The degree of the concave or convex bow-out is directly related to

the magnitude of the stress. The curvature, κ , is calculated from the measured maximum displacement of the plate, d , by

$$\kappa = \frac{8d}{4d^2 + L^2} \quad (1)$$

where L is the original length of the plate as shown in Figure 1.

The intrinsic stress of electroless Ni-P film can be calculated from the curvature of the composite plate by [5]:

$$\sigma_f = \frac{1 + \frac{E_f(1-\nu_s)\left(\frac{h_f}{h_s}\right)^3}{E_s(1-\nu_f)\left(\frac{h_f}{h_s}\right)}}{1 + \frac{h_f}{h_s}} \frac{E_s h_s^2}{6(1-\nu_s)h_f} \kappa \quad (2)$$

where E , ν , and h are Young's modulus, Poisson's ratio and thickness. The subscript "s" and "f" stand for substrate and the deposited film, respectively. It has to be pointed out that the calculated stress is an average value through the film thickness. It has to be emphasized that in our study this simple approach is effective enough for the average stress, but not for the stress variation through thickness. The stress value obtained from the curvature measurement carried out at room temperature is a combined result of intrinsic stress and thermal stress. The effect from thermal stress can be estimated by knowing the difference in temperature between plating temperature and the room temperature when the measurement are made, and the difference in the coefficient of thermal expansion for Ni-P and Cu. For this purpose we assume room temperature is 25°C, and the CTEs for Ni-P and Cu are taken as $13 \times 10^{-6}/^\circ\text{C}$ and $17 \times 10^{-6}/^\circ\text{C}$, respectively. Since the CTE for Ni-P is low, when cooling down from higher temperature the strain induced in the Ni-P should be compressive. Finally the reported

intrinsic stresses in Ni-P below are the ones after the influence from thermal stress has been calibrated.

Cross-sections of electroless Ni-P deposits were obtained by electro-etching. The morphology of Ni-P was investigated with scanning electron microscopy (SEM). X-ray diffractometry (XRD) was used to analyse the crystallinity of the Ni-P. An analysis of variables experiment of 3 factors (pH value, accumulated salt, and surface roughness) with 3 different levels ($3 \times 3 \times 3$) orthogonal experiment was carried out to identify the influence of each key factor and their compound effects. The ANOVA ($3 \times 3 \times 3$) orthogonal matrix is shown in Table 1. The factors selected for this investigation and the levels are listed in Table 2.

In the current study, Na_2SO_4 and NaH_2PO_3 were added to simulate the actual salt accumulation through number of metal turnover (MTO). From the EN plating recipe, the consumption of 2 mol NaH_2PO_2 can reduce 0.7 mol of Ni^{2+} . Therefore in this investigation, the molecular ratio of Na_2SO_4 and NaH_2PO_3 added was kept at the constant ratio of 7:20.

3. Results and discussion

3.1 Analysis of variance on intrinsic stress

Twenty-seven experiments were carried out to investigate the average deposit stress as a function of pH value, accumulated salt, and surface roughness. The summary results of the intrinsic stress are listed in Table 3. In table 4 d.f. denotes the degree of freedom, SS the sum of square of variables, MS the mean sum of square of variables, F the F-statistic observe value and $F(0.05)$ the F-statistic critical value. According to ANOVA, the pH value and side products (Na_2SO_4 , and NaH_2PO_3) greatly influence the intrinsic stress. These two variables also have significant compound effect on the formation of EN intrinsic stress during the

plating process. Meanwhile, neither the factor of surface roughness nor its compound effects with other variables influences the stress significantly.

The summary of the experimental results is also shown in Figure 2. Tensile stresses increased with increasing the pH value even in fresh solution. A summary inspection of the results also showed that the intrinsic stresses for fresh solution were very low tensile. In the aged solution, the tensile stress increased. Salt content and pH value had a compound effect on the intrinsic stress of EN film. When the pH value was low (pH 4.5, 4.9), there was not much difference in the Ni-P intrinsic stress between fresh solution and aged one. At higher pH value (pH 5.3), aged solution had a greater influence on the intrinsic stress. The intrinsic stress of solution aged in level 3 was relatively high, while the stress of fresh solution was relatively low.

In Figure 3 the deposition rate was plotted with the intrinsic stress. Higher deposition rate corresponded to higher intrinsic stress in the Ni-P coating. Combining the results in Figure 2 and Figure 3, it seems to suggest that the high deposition rate and high salt concentration are related to high level of intrinsic stress. However micro-structural investigation is necessary before any further analysis can be made.

3.2 Ni-P microstructure

The cross-section of Ni-P deposit plated under different operating parameters is selectively shown in Figure 4 and 5. They actually represent two extremes of the intrinsic stresses found in this experiment: Figure 4 is the one deposited at pH 4.8 with fresh solution which had 50 MPa tensile stress. Figure 5 shows the one deposited at pH 5.3 with level 3 of salt concentration that resulted in higher tensile stress (180 MPa). The morphology of cross-section of EN deposit showed a pronounced difference. Both had banded or lamellar structure, but for the low-stress case (Figure 4) there were few layers through the thickness of EN deposit while the contrast between layers was higher.

The lamellar structure of Ni-P deposit can be attributed to compositional variations with deposit thickness. Therefore the higher inter-lamella contrast (verified by the gray scale measurement but not shown in this paper) in Figure 4 indicates a higher fluctuation in P content. The cause of the compositional variation could be explained by the periodical fluctuation in the pH of the plating solution adjacent to the deposit surface and the fact that the co-deposition of P with Ni is very sensitive to the fluctuation of the pH value. The fluctuation in pH is caused by hydrogen evolution and the reduction of hypophosphite, which decreases the pH value. It takes time for the solution at the “local” metal/solution interface to return back to the composition of the bulk through diffusion. For the high pH solution, the reaction rate is relatively high which leads to fast deposition rate. Due to the high $[H^+]$ releasing rate, the variance of the pH adjacent to the reaction surface is more rapid, and the hydrogen bubbles are created fast. These bubbles can effectively stir up the solution so that the lamellar structure tends to be smoother.

From the SEM observation, markings perpendicular to the lamellar structure could also be observed (Figure 6). This structure was different from the columnar structure exhibited by electrolytic deposition. It could be seen that the columns in current work corresponded to the surface unevenness (cf. Figure 4-6) at the beginning of the deposition. Later some columns merged to form wider ones. It was very tempting to correlate the surface roughness and the resulting columnar structure with the intrinsic stress formation. However, a statistical study did not find any significant effect of surface roughness on the intrinsic stresses. This seemed to suggest that the columnar structure in electroless deposits its might not be the root cause of intrinsic stress, at least for the range of roughness investigated.

The development of the intrinsic stress is a consequence of diffusion effect in previously deposited section of the film. Early work [6] explained the formation of intrinsic stress as a result of constrained grain boundary relaxation. The magnitude of resulting strain could be

estimated by the ratio of grain boundary relaxation distance over the average grain diameter. More recently Sheldon et al [7] suggested that both the film surface roughness during the very early stage of film growth and subsequent grain boundary formation were responsible for the intrinsic stresses generated at different stage. Their study was based on the experiment with CVD crystalline diamond films. Mayr and Samwer [8] used $Zr_{65}Al_{7.5}Cu_{27.5}$ to study the intrinsic stress in amorphous coatings where the coating surface morphology was observed under scanning tunneling microscope. They proposed a model based on local energy minimization of the surface to account for the tensile intrinsic stress in amorphous thin films.

Regardless of the difference in proposed mechanisms and therefore the corresponding models used, the formation of intrinsic stress involves mechanisms that eliminate defects associated with free volume. The defects include grain boundaries, vacancies, interstitial voids and gas molecules. Diffusion allows the density of previously created defects to be reduced by grain growth, or dislocation climb, annihilation, etc. For a film constrained in-plane, misfit arises as the film attempts to either contract or expand. It is not unreasonable to argue that high deposition rate in current work tends to generate more such “defects”, especially when the solution deteriorates with accumulated salts. As a result, the intrinsic stress measured was higher.

3.3 Effect of annealing

Low temperature annealing at 150°C and 190°C were performed after Ni-P deposition. Stress was calculated and analyzed by ANOVA method. After aging at 190°C for 170 hours, the average residual stresses of Ni-P deposits were shown in Figure 7. Compared with the results without annealing in Figure 2, there was no significant difference between the two cases. DSC experiments (Figure 8) on the as-deposited, annealed at 150°C and 190°C samples showed there was no phase transformation for neither of them before 340°C. It has been shown by many previously that Ni_3P crystalline phase begins to form around 340°C [9].

XRD patterns of these Ni-P coatings were shown in Figure 9. The single broad peak indicated an amorphous phase at the as-deposited coatings as well as in the annealed samples at 150°C and 190°C. The reason we called the structure amorphous rather than nanocrystalline is because that in current study the breadth at the half peak for all three cases was very broad (between 4 and 5°). Therefore it is more justifiably to classify them as amorphous, not nanocrystalline. Still some difference among the three cases could be observed: the peak of Ni-P annealing at 190°C was sharper than that of as-deposited. Such result correlated well with the DSC experiments (Figure 9) where the peak of 190°C annealed sample was lower than that of the as-deposited one. This suggested that certain degree of atomic re-arrangement at short distance scale might have happened during annealing but at a long distance scale the structure was still overwhelmingly amorphous. From our experimental results, intrinsic stress was not significantly affected by annealing up to 190°C. This seemed to indicate that the mobility of atoms at low temperature was not enough to cause defect annihilation. Microstructure analysis also indicated that there was virtually no change in the lamellar structure after annealing, which was a good indication that the long distance diffusion had not happened yet.

4. Conclusion

Not only pH value and aged solution, but also their compounding effects have significant influence on the intrinsic stress in the electroless nickel (EN) deposition. However, the surface roughness does not have significant effect on the intrinsic stress at the range studied. The higher the solution pH value and the more the number of solution metal turnover MTO, the higher the tensile stress developed in the Ni-P deposit. After aging up to 190°C for 170 hours, the intrinsic stress largely remained the same. Microstructural analysis recorded a slight change in its crystallinity but the change is not great enough to cause significant variation in intrinsic stresses.

Acknowledgement

Financial support of this work from Nanyang Technological University under AcRF grant 00/19 is gratefully acknowledged.

References:

- [1] Dianne Mitchell, Yifan Guo, and Vijay Sarihan, Methodology for Studying the Impact of Intrinsic Stress on the Reliability of the Electroless Ni UBM Structure, IEEE Transactions on Components and Packaging Technologies, 24 (2001), p667-672
- [2] Chun-Jen Chen and Kwang-Lung Lin, Internal Stress and Adhesion of Amorphous Ni-Cu-P Alloy on Aluminium, Thin Solid Films, 370 (2000), p106-113
- [3] R. N. Duncan, The Effect Of Solution Age On Corrosion Resistance Of Electroless Nickel Deposits, Plating and Surface Finishing, 10 (1996), p64-68
- [4] Alberto Garcia-Diaz and Don T. Phillips, Principles of Experimental Design and Analysis, Chapman & Hall, 1995
- [5] A. G. Evans and J. W. Hutchinson, The Thermomechanical Integrity of Thin Films and Multilayers, Acta Metallurgica et Materialia, 43 (1995), p2507-2530
- [6] F. A. Doljack and R. W. Hoffman, The Origins of Stress in Thin Nickel Films, Thin Solid Films, 12 (1972), p71-74
- [7] B. W. Sheldon, K. H. A. Lau and A. Rajumani, Intrinsic Stress, Island Coalescence, and Surface Roughness during the Growth of Polycrystalline Films, Journal of Applied Physics, 90 (2001), p5097-5103
- [8] S. G. Mayr, and K. Samwer, Model for Intrinsic Stress Formation in Amorphous Thin Films, Physical Review Letters, 87 (2001), 036105
- [9] G. O. Mallory and J. B. Hajdu, Electroless Plating – Fundamentals and Applications, (1990), American Electroplaters & Surface Finishers Society

List of Tables:

Table 1. ANOVA matrix of (3×3×3).

Table 2. Factors studied for intrinsic stress in EN plating

Table 3. As-deposit (before annealing) intrinsic stresses

Table 4. Analysis of variables for the intrinsic stresses

List of Figures:

Figure 1. Strip deflection caused by a thin film subject to intrinsic stress

Figure 2. Intrinsic stress of Ni-P deposit as a function of pH and salt concentration

Figure 3. Intrinsic stress v.s. deposition rate

Figure 4. Cross-section of Ni-P deposited in fresh solution, pH 4.9 (BSI)

Figure 5. Cross-section of Ni-P deposited in aged solution, pH 5.3 (BSI)

Figure 6. Surface roughness induced columnar structure

Figure 7. Intrinsic stress of Ni-P deposit after 170 hour annealing at 190°C

Figure 8. DSC results of Ni-P at different aging temperatures for 170 hours

Figure 9. XRD results of Ni-P deposits annealed at different temperatures for 170 hours. (a) room temperature (b) 150 °C (c) 190 °C

No	pH	salt	surface	No	pH	salt	surface	No	pH	salt	surface
	1	1	1		2	1	1		3	1	1
	1	1	2		2	1	2		3	1	2
	1	1	3		2	1	3		3	1	3
	1	2	1		2	2	1		3	2	1
	1	2	2		2	2	2		3	2	2
	1	2	3		2	2	3		3	2	3
	1	3	1		2	3	1		3	3	1
	1	3	2		2	3	2		3	3	2
	1	3	3		2	3	3		3	3	3

Table 1

Factors	1	2	3
Level	pH value	Accumulated salt (M) (Na ₂ SO ₄ + Na ₂ HPO ₃)	Surface roughness (Ra)
1	4.5	0.00 + 0.00	Electropolished 509±229/200 Å
2	4.9	0.10 + 0.28	As-received 1090±275/174 Å
3	5.3	0.20 + 0.56	Etched 2871±434/205 Å

Table 2

Experiment No.	1.	2.	3.	4.	5.	6.	7.	8.	9.
Condition (pH-salt-surface)	1-1-1	1-1-2	1-1-3	1-2-1	1-2-2	1-2-3	1-3-1	1-3-2	1-3-3
Intrinsic stress treatment 1 (MPa)	22.6	48.5	61.6	65.2	49.3	51.1	59.8	67.5	60.7
Intrinsic stress treatment 2 (MPa)	45.5	38.2	67.3	56.6	44.0	46.9	55.2	49.9	66.0
Experiment No.	10.	11.	12.	13.	14.	15.	16.	17.	18.
Condition (pH-salt-surface)	2-1-1	2-1-2	2-1-3	2-2-1	2-2-2	2-2-3	2-3-1	2-3-2	2-3-3
Intrinsic stress- treatment 1 (MPa)	50.7	84.1	64.2	53.1	70.2	55.2	102.3	94.7	76.4
Intrinsic stress treatment 2 (MPa)	55.2	72.5	52.4	46.2	57.1	52.9	71.9	70.8	80.5
Experiment No.	19.	20.	21.	22.	23.	24.	25.	26.	27.
Condition (pH-salt-surface)	3-1-1	3-1-2	3-1-3	3-2-1	3-2-2	3-2-3	3-3-1	3-3-2	3-3-3
Intrinsic stress- treatment 1 (MPa)	72.4	69.3	78.3	92.4	100.5	73.2	136.3	113.5	180.9
Intrinsic stress treatment 2 (MPa)	55.9	69.8	64.2	70.8	77.5	66.9	102.7	127.5	118.2

Table 3

source	df	SS	MS	F	F(0.05)	Significance
pH	2	14553.4	7276.7	39.57	3.35	yes
salt	2	10652.6	5326.3	28.97	3.35	yes
pH-salt	4	4952.0	1238.0	6.73	2.73	yes
roughness	2	346.0	173.0	0.94	3.35	
Rough-pH	4	711.3	177.8	0.97	2.73	
rough-salt	4	1021.6	255.4	1.39	2.73	
pH-salt-roughness	8	1742.1	217.8	1.18	2.31	
Error	27	4964.6	183.9			

Table 4

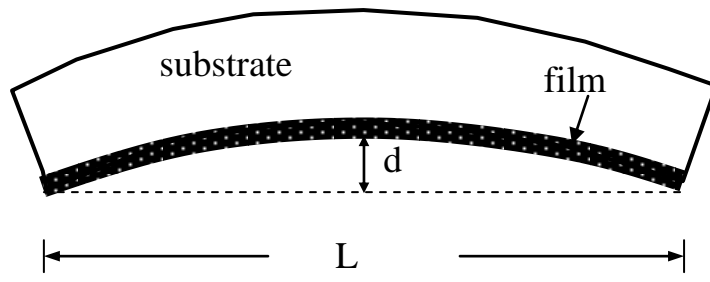


Figure 1

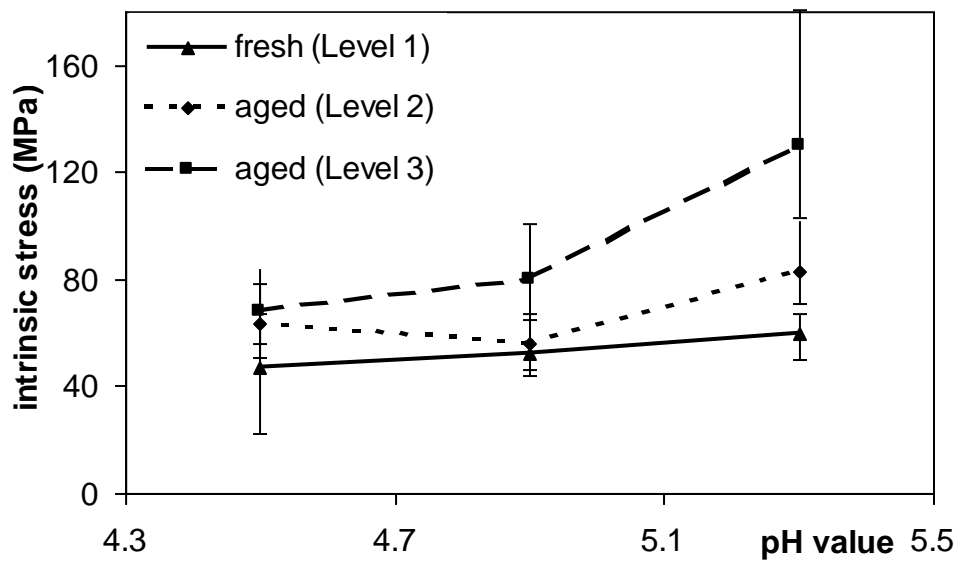


Figure 2

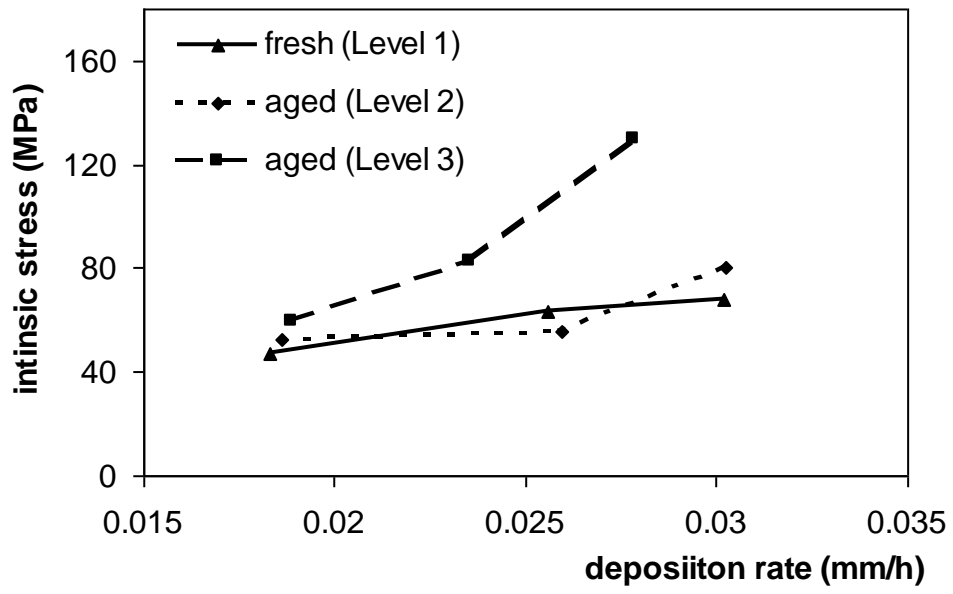


Figure 3

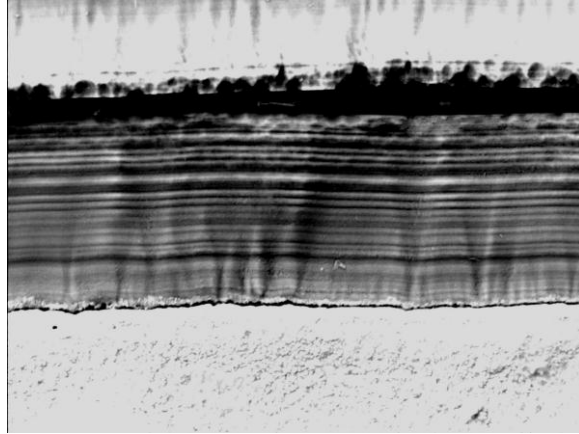


Figure 4

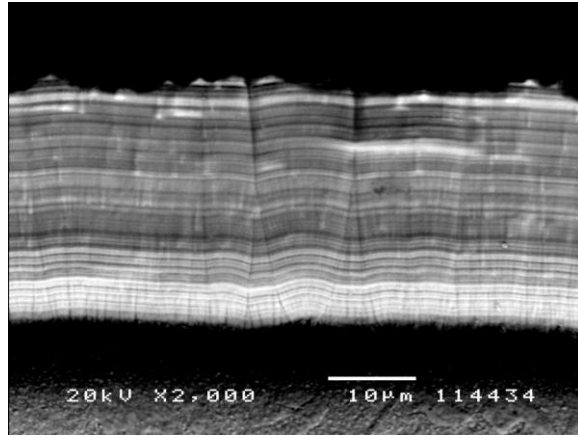


Figure 5

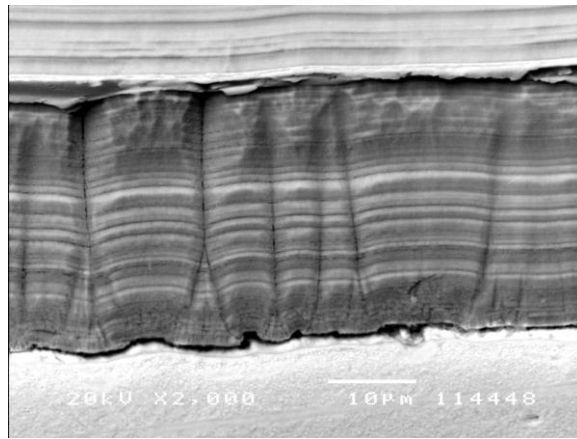


Figure 6

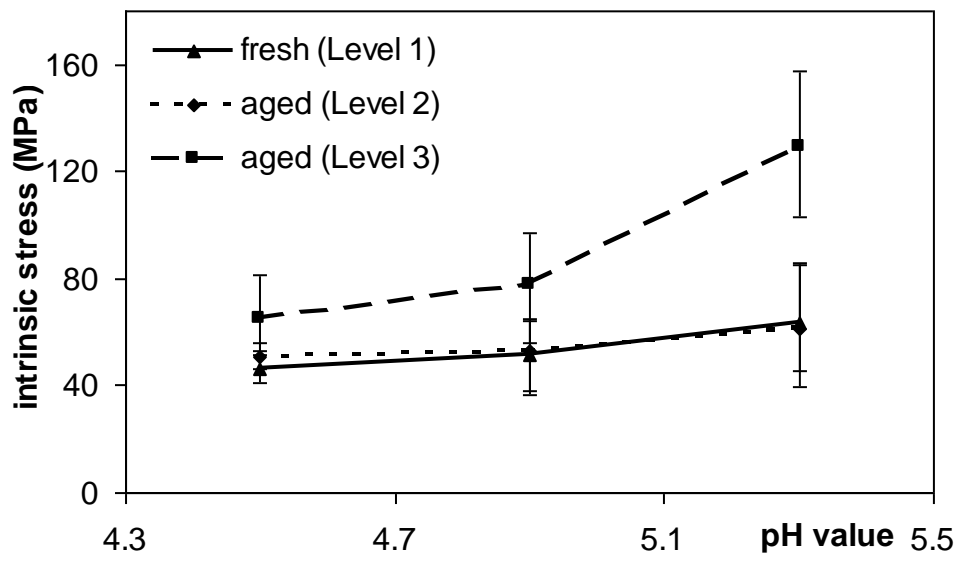


Figure 7

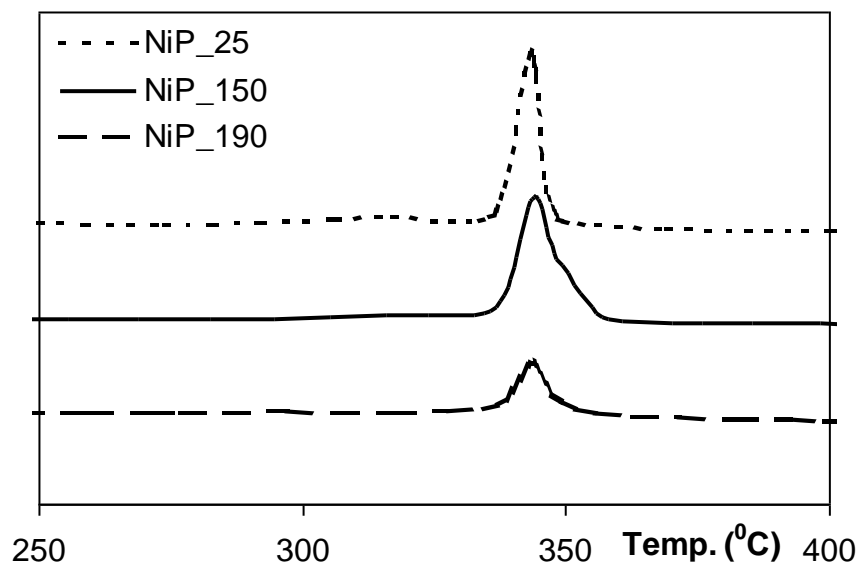


Figure 8

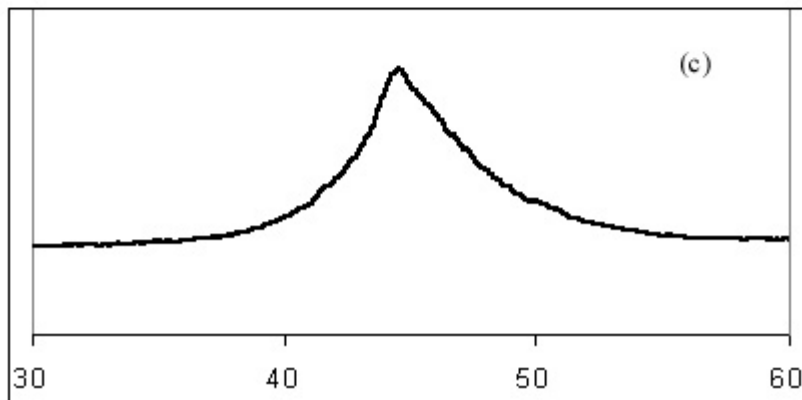
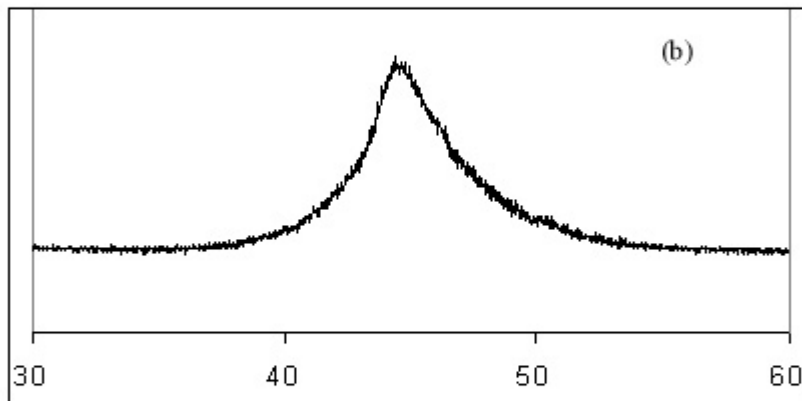
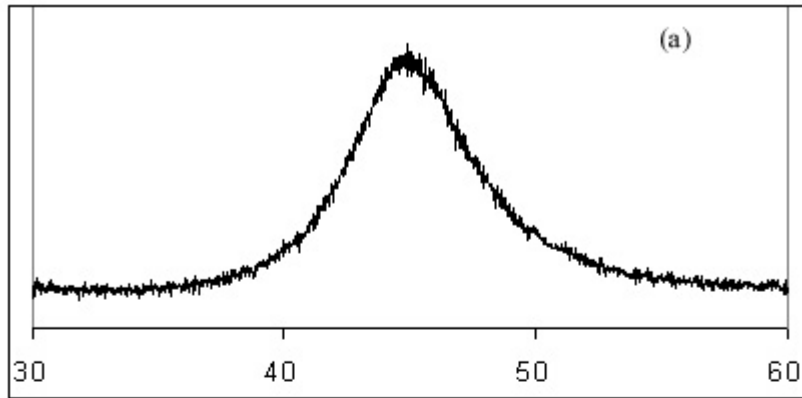


Figure 9